Tectonic history of a Jurassic backarc-basin sequence (the Gran Cañon Formation, Cedros Island, Mexico), based on compositional modes of tuffaceous deposits

Salvatore Critelli*
Dipartimento di Scienze della Terra, Università degli Studi della Calabria, 87036 Arcavacata di Rende (CS), Italy

Kathleen M. Marsaglia[†]
Department of Geological Sciences, California State University, Northridge, California 91330-8266, USA

Cathy J. Busby[§]
Department of Geological Sciences, University of California, Santa Barbara, California 93106, USA

ABSTRACT

The Jurassic Gran Cañon Formation (Cedros Island, Baja California, Mexico) constitutes an unusually well preserved and exposed example of ancient backarc-basin fill. Petrofacies analysis conducted on tuffaceous sandstone and tuff samples from this formation complement and reinforce prior lithofacies interpretations, but with some modification. When temporal and spatial trends in petrographic data (detrital modes) are analyzed and compared to models based on data collected from Deep Sea Drilling Project and Ocean Drilling Program cores, the trends indicate a second, heretofore unrecognized, phase of backarc rifting. Basalt lavas interstratified with dacitic pyroclastic rocks of the primary volcanic lithofacies, previously interpreted to record the eruption of differentiated magmas at the climax of growth of the Gran Cañon island arc, are now as a result of this study considered to be the product of arc extension and rifting.

Our method of modal analysis uniquely combines the quantification of textural attributes of pyroclastic and epiclastic debris that reflect eruption style and magma composition, as well as the effects of reworking and mixing in marine settings. This study demonstrates that detailed petrographic analysis is useful in the interpretation of ancient volcaniclastic deposits suspected of having formed in backarc-basin settings.

Keywords: backarc basins, Baja California, Jurassic, magmatic arcs, Mexico, provenance, sandstone petrology, volcanology.

INTRODUCTION

Few detailed studies have been conducted on ancient, uplifted, intraoceanic backarc-basin assemblages, probably because of their intraoceanic setting and poor preservation during subduction and terrane accretion. The volcaniclastic fill of a late Middle Jurassic backarc basin on Cedros Island (Baja California) (Fig. 1), the Gran Cañon Formation, is remarkable for its low degree of structural modification, its low to moderate alteration and metamorphism, and its unusually good exposure. Detailed facies analysis of this backarc basin was previously conducted by Busby-Spera (1987, 1988). In this paper, we present new petrographic data from the Gran Cañon Formation and compare these with petrographic data from modern backarc basins We refine the earlier-published model for the tectonic evolution of the Jurassic arc-backarc system on Cedros Island. In this refined model, we infer that a second phase of arc rifting has been recorded in the backarc-apron sequence (subsequent to the phase that formed the basin). The second rifting event resulted in conversion of the active backarc basin into a remnant backarc basin.

Our petrographic methods include modal analysis designed to quantify the textural attributes of pyroclastic and epiclastic debris that reflect eruption style, in addition to those that relate to magma composition. The modal analysis of textures makes use of descriptive classes of shard morphology commonly referred to by volcanologists (e.g., Heiken and Wohletz, 1985) in SEM (scanning electron microscope) studies and only recently quantified in modal analysis of lithified rocks by De Rosa (1999). The modal analysis of magmatic components to determine their composition was developed by sedimentary petrologists (e.g., Dickinson, 1970; Ingersoll and Cavazza, 1991; Marsaglia, 1992, 1993; Critelli and Ingersoll, 1995; Marsaglia and Devaney, 1995) to help fingerprint mafic, intermediate-composition, and felsic components and their relative proportions in reworked tuffaceous sediments. To quantify these parameters in combination provides a unique approach to interpreting the provenance of pyroclastic sediments deposited in marine settings, where reworking and mixing can be common processes.

Results from the Deep Sea Drilling Project (DSDP) and Ocean Drilling Program (ODP) have greatly improved our understanding of backarc-basin facies relationships and sediment provenance (Karig, 1983; Taylor and Karner, 1983; Klein and Lee, 1984; Klein, 1985; Nishimura et al., 1991; Klaus et al., 1992; Tappin et al., 1994; Arculus et al., 1995; Cambray et al., 1995; Clift, 1995; Clift and ODP Leg 135 Scientific Party, 1995; Hawkins, 1995; Marsaglia, 1995; Marsaglia et al., 1995). However, these widely spaced drill holes provide only a limited view of largely submerged, tectonically complex basins, leav-

*E-mail: critelli@unical.it.
[†]E-mail: Kathie.marsaglia@csun.edu.
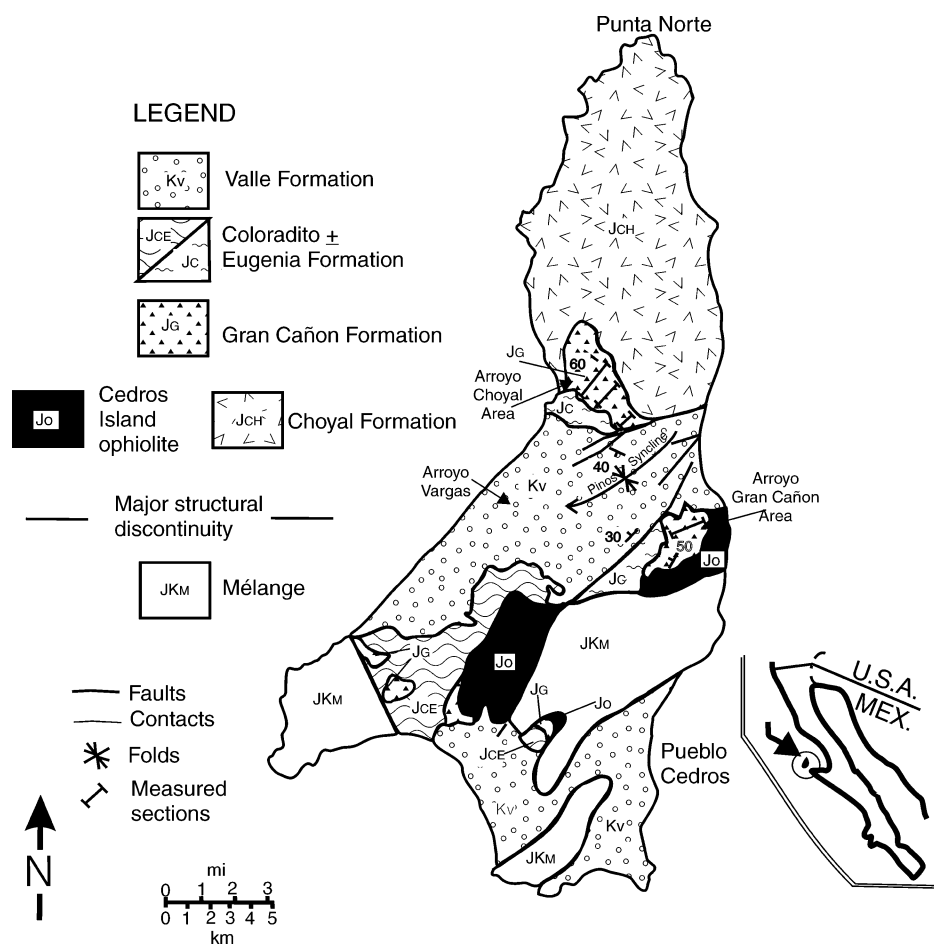[§]E-mail: Cathy@magic.geol.ucsb.edu.

Figure 1. Generalized geologic map of Cedros Island (modified from Kilmer, 1977, 1984) and location of the measured sections shown in Figure 2.

ing much to learn about facies and depositional processes in these settings. Our new petrographic data complement the data set from modern basins by documenting the evolution of a backarc apron in a more arc-proximal setting than most of the drill sites in the western Pacific. Proximal coarse-grained volcaniclastic packages, such as the Gran Cañon Formation, provide more detailed information on the tectonic and volcanic evolution of an intraoceanic arc during backarc-basin formation (Marsaglia and Devaney, 1995).

GEOLOGIC AND STRATIGRAPHIC SETTING OF THE GRAN CAÑON FORMATION

A rifted-arc and ophiolite assemblage and overlying volcaniclastic rocks, all of late Middle Jurassic age, represent a fragment of the arc side of a backarc basin, now exposed on Cedros Island in Baja California (Kilmer, 1977, 1984; Kimbrough, 1984; Busby-Spera, 1987, 1988; Fig. 1). Backarc ophiolite gener-

ation was immediately followed by progradation of a deep-water pyroclastic apron into the backarc basin, contemporaneous with the growth of an oceanic arc from deep water to sea level or above. Busby-Spera (1987, 1988) divided this pyroclastic apron into *tuff, lapilli tuff–tuff breccia,* and *primary volcanic* lithofacies (Fig. 2). Whole-rock analyses and microprobe studies show that the basalts in the primary volcanic lithofacies are chemically and petrographically homogeneous tholeiitic basalts that are distinctly more alkalic than tholeiitic rocks of the ophiolitic or arc basement to the Gran Cañon Formation (Kimbrough, 1982, 1984). The pyroclastic apron was then blanketed by a relatively thin sheet of siltstone to fine-grained sandstone turbidites (*"epiclastic lithofacies"*; Fig. 2), interpreted to record abrupt extinction and erosion, but no uplift, of the island arc within 10 m.y. of ophiolite generation. This cycle was inferred to reflect the episodic nature of processes in backarc basins (Busby-Spera, 1988),

which appear to form in 10 m.y. or less (Taylor and Karner, 1983).

METHODS

Volcaniclastic Terminology

Volcaniclastic units in the Gran Cañon Formation are composed of sand pyroclasts and matrix that are inferred by their textural attributes and sedimentary structures to have been transported and deposited in a submarine environment by turbidity currents. If a classification scheme based on transport and depositional processes (McPhie et al., 1993) is used, these samples would be called sandstones. According to a classification scheme based on the origin of the particles (Fisher and Schmincke, 1984), however, these samples would be called tuffs because they are mostly composed of compositionally homogeneous pyroclasts that show little to no textural modification. Therefore, as described in the previous section and as shown in Figure 2, these deposits are referred to as tuffs, but for purposes of comparison with modern backarc-basin deposits described in the literature, they are referred to as *tuffaceous sandstones*.

Petrographic and Modal Analysis

We selected 32 medium- to coarse-grained tuffaceous sandstone samples from the Gran Cañon Formation for thin-section preparation and modal analysis. These cover the entire formation in both proximal and distal sections (Fig. 2; Table DR1[1] presents field description of samples used for petrographic study and lithofacies subdivision of Gran Cañon Formation). We also examined thin sections of lithic blocks from the tuff breccias, as well as thin sections of basalt lava flows, to characterize better the mineral assemblages and textures of smaller fragments within the tuffaceous sandstones. Some thin sections were etched and stained for plagioclase and potassium feldspar.

The tuffaceous sandstone samples were point-counted through the use of a petrographic microscope equipped with an automated stage. Five hundred points were counted for each sample by using the Gazzi-Dickinson method (Ingersoll et al., 1984; Zuffa, 1985, 1987). Grain parameters (Zuffa, 1985, 1987; Critelli and Le Pera, 1994) are defined and
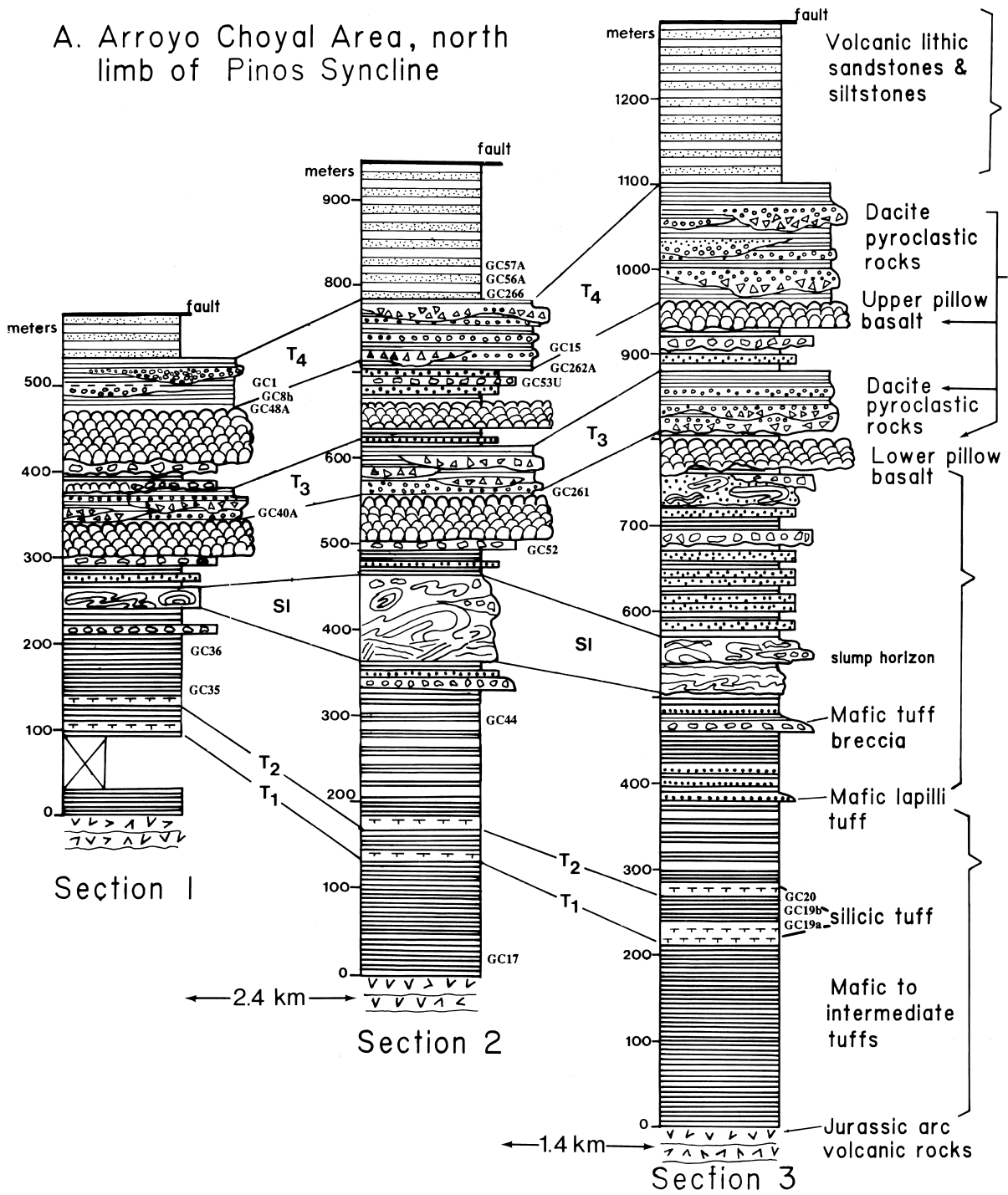
Figure 2. (A–C) Measured sections of the Gran Cañon Formation, Cedros Island (modified from Busby-Spera, 1988). Localities of sections A (1, 2, 3), B, and C are plotted in Figure 1. (D) Paleocurrent data indicate a northern source for the Gran Cañon Formation, and pyroclastic debris coarsens toward the inferred northern source area (from C to B to A). Felsic tuffs T1 to T4 and slumping horizon Sl are marker horizons. GC1 to GC266k refer to samples used for petrographic study (Tables DR1, DR2, and DR3—see footnote 1). See Busby-Spera (1987, 1988) for descriptions and interpretations of the stratigraphy.
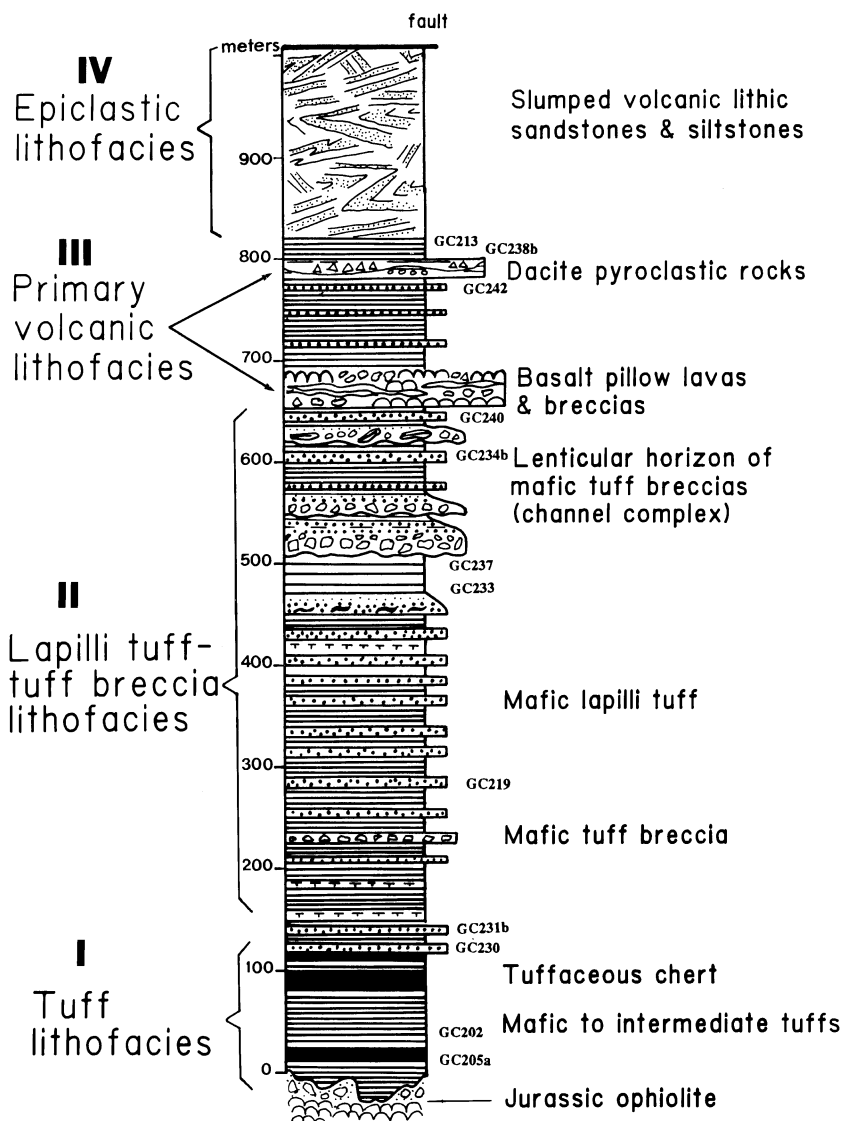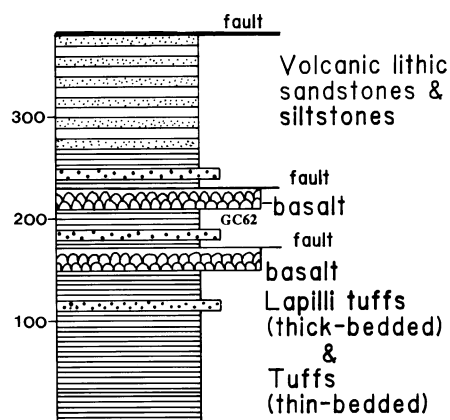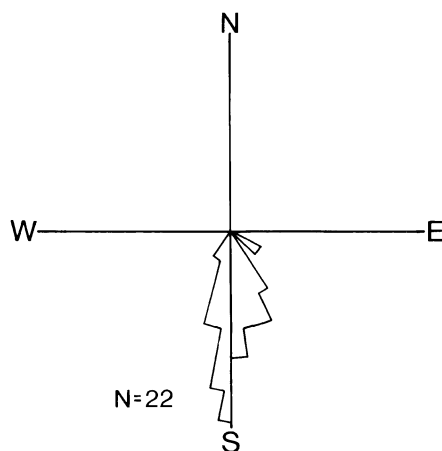
Figure 2. (*Continued.*)

raw point-count data are presented in Table DR2 (see footnote 1), whereas recalculated modal point-count data are defined and presented in Table DR3 (see footnote 1). Grain parameters for the volcanic grains are those of Dickinson (1970), Marsaglia (1993), and Critelli and Ingersoll (1995), modified to include information on grain shape and fragment morphology (e.g., blocky, scoria, bubble wall; similar to the scheme outlined in De Rosa [1999]). The types of glassy material (e.g., blocky vs. bubble-wall shards, Table DR2), as well as the degree of rounding of fragile and resistant grains (e.g., glass vs. crystals or lithic fragments), provide valuable information for inferring eruptive styles and transport histories. Note that in the thin sections that were not stained, some zeolitized grains may have been inadvertently included in the felsitic category.

PETROGRAPHIC DESCRIPTIONS

Basalt Lava Flows

Phenocrystic phases in thin sections of basalt lava flows include plagioclase (dominant-ly labradorite and bytownite-labradorite by optical determination), clinopyroxene as diopside (optically determined), and iron-titanium oxides. By using the textural subdivision of volcanic rocks of Williams et al. (1954), the basalts show intersertal, intergranular, and hyalophitic textures.

Dacite Blocks

Phenocrystic phases in dacite blocks include plagioclase (zoned from labradorite-andesine to oligoclase by optical determina-

tion), green hornblende, minor quartz, and rare potassium feldspar. Groundmass minerals include plagioclase, quartz, hornblende, and magnetite. The dominant groundmass texture is felsitic granular, consisting of an anhedral microcrystalline mosaic composed mainly of quartz and feldspar with uniform, very fine grain size. Hyalopilitic texture in which colorless glass occupies the minute interspaces between randomly oriented microlites of plagioclase is also common. In some cases, this glass is largely recrystallized. Vitrophyric texture in which phenocrysts lie in a matrix of glass (with or without minor alteration and/or devitrification of the glass) also occurs.

Volcaniclastic Sandstone

Most samples come from graded beds, or upward-fining and upward-thinning sequences of beds interpreted as turbidites (Table DR1—see footnote 1). The samples are poorly sorted, and the clasts are largely angular, although rare subangular to subrounded grains occur in most samples. They exhibit a range of compositions, from mafic to intermediate to felsic. Volcanic lithic fragments are the dominant component. The rare nonvolcanic grains consist solely of intrabasinal carbonate bioclasts and intraclasts. Crystals, counted as monocrystalline grains, are all euhedral. In the felsic samples, they are dominantly zoned plagioclase (andesine-labradorite to oligoclase) with lesser quartz and hornblende, and rare potassium feldspar. The intermediate-composition to mafic samples have plagioclase (bytownite to labradorite) and clinopyroxene crystals. Accessory detrital minerals include (in decreasing order of abundance) magnetite and epidote in the more mafic samples, and ilmenite, epidote, magnetite, and rare apatite in the more felsic samples.

Interstitial materials within the Gran Cañon Formation samples include detrital matrix and authigenic cement. Detrital matrix is represented by very fine volcanic ash, but it is difficult to estimate original abundances because the degree of recrystallization or replacement varies from sample to sample; therefore, only minimum estimates of original ash matrix can be made by using present abundances. These are 0–1.6% for the mafic samples and 0–13.6% for the felsic samples (Table DR2—see footnote 1). Calcite cement is present in all of the mafic samples (6%–51%) and includes pore-filling (0%–23%) and poikilotopic (0–47.6%) types. Authigenic silica, laumontite, heulandite, and clay minerals serve as minor (0%–7%) cements (Table DR2). Authigenic silica cement is present in the felsic samples

(0%–32%), and calcite is rare (0%–16%), except for one sample with abundant late poikilotopic cement (GC242, 16%); authigenic clay minerals (0–6.4%), zeolites (laumontite and heulandite; 0–4.8%), and albite (0–0.8%) are subordinate (Table DR2).

Lithic Fragment Types in Tuffaceous Sandstone

Volcanic lithic grains in Gran Cañon samples of intermediate to mafic composition are variably devitrified and altered to clay minerals and zeolites; they show lathwork, microlitic, and vitric textures (Fig. 3). Volcanic lithic fragments in Gran Cañon felsic samples show predominantly felsitic granular and vitric textures with rare microlitic volcanic lithic grains.

Lathwork volcanic lithic fragments (Lvl; see Figs. 3 and 4), as first defined by Dickinson (1970), have sand-sized phenocrysts in a groundmass of glass or devitrified glass (Fig. 3, A and B). This texture is characteristic of basaltic and basaltic andesite lavas and pyroclasts. In the more mafic samples from the Gran Cañon Formation, the phenocrysts are laths of labradorite plagioclase and clinopyroxene, and the glassy groundmass is black, brown or orange, or is microlitic (see subsequent discussion). These lathwork volcanic lithic grains are similar in texture to the groundmass of both intergranular and hyalophitic textures in the basalt lava flows.

Microlitic volcanic lithic fragments (Lvmi; see Figs. 3 and 4) are defined as fragments that contain variable amounts of microlites of plagioclase or ferromagnesian minerals that are visible at high magnification and are <0.0625 mm long (Dickinson, 1970). Microlitic texture is typical of andesites, but it also commonly occurs in basalts and basaltic andesites. In Gran Cañon samples, plagioclase microlites occur in a dominantly black, brown (Fig. 3C), or orange vitric groundmass. The microlitic texture in the tuffaceous sandstone samples is similar to the interstices of intergranular and hyalophitic textures in the basalt lava flows. Felsic microlitic fragments are rare and consist of pumice fragments with microlites of plagioclase.

Vitric volcanic lithic fragments (Lvv; see Figs. 3 and 4) are defined as pumice or scoria and glass shards, but also include partially to wholly altered glass (Dickinson, 1970; Ingersoll and Cavazza, 1991; Marsaglia, 1992). Volcanologists refer to these as vitric fragments, rather than vitric lithic fragments, in order to distinguish them from nonglassy fragments, which they call lithic fragments. Every

sample has either blocky shards (of hydroclastic origin) or scoria fragments (of explosive magmatic origin) (Table DR2—see footnote 1), and some of the scoria fragments are blocky in shape (indicating phreatomagmatic eruptions, Heiken and Wohletz, 1985). The glass in Gran Cañon mafic tuffaceous sandstone samples is sideromelane (i.e., light brown colored), but most of these grains are at least partially altered to clay or zeolite minerals (Fig. 3, C–E). Palagonite alteration is dominant, accompanied in some samples by lesser montmorillonite and minor laumontite. Orange, brown, and black vitric lithic fragments in Gran Cañon tuffaceous sandstone samples are similar to glassy material in the groundmass of intergranular-, hyalophitic-, and intersertal-textured basalt lavas that are interbedded with the tuffaceous sandstone. Vitric volcanic lithic fragments (Lvv) in the felsic samples are colorless and consist of bubble-wall shards and pumice (Fig. 3H).

Felsitic volcanic lithic fragments (Lvf) may include two types, granular and seriate (Dickinson, 1970; Ingersoll and Cavazza, 1991). Felsitic granular texture consists of anhedral microcrystalline mosaics, with uniform, very fine grain size, composed mainly of feldspar and quartz and/or mafic minerals. Vitric grains may grade into granular grains through devitrification. Felsitic granular texture is typical of rhyolites and dacites (Ingersoll and Cavazza, 1991). Felsitic seriate texture is an anisometric mosaic, with a wide range of crystal sizes and shapes, composed mainly of feldspar, quartz, and/or mafic minerals. Felsitic seriate texture is typical of dacites and andesites (Ingersoll and Cavazza, 1991). Seriate felsitic fragments are rare in Gran Cañon samples, and granular felsitic grains are abundant, suggesting that they are silicic rather than intermediate in composition. In addition, the dominance of plagioclase and hornblende (Fig. 3, F and G), rather than potassium feldspar and quartz phenocrysts, suggests a dacitic, rather than rhyolitic, composition for these fragments.

COMPOSITIONAL MODES AND PETROFACIES OF THE GRAN CAÑON FORMATION

The Gran Cañon samples are feldspatholithic, plotting along the base of a standard Qm-F-Lt ternary diagram (Fig. 4A) used for tectonic-provenance analysis of sandstones (e.g., Dickinson and Suczek, 1979; Dickinson, 1982, 1985, 1988). Table DR4 (see footnote 1) shows recalculated average vitric, microlitic, lathwork, and felsitic volcanic lithic grains of published volcaniclastic
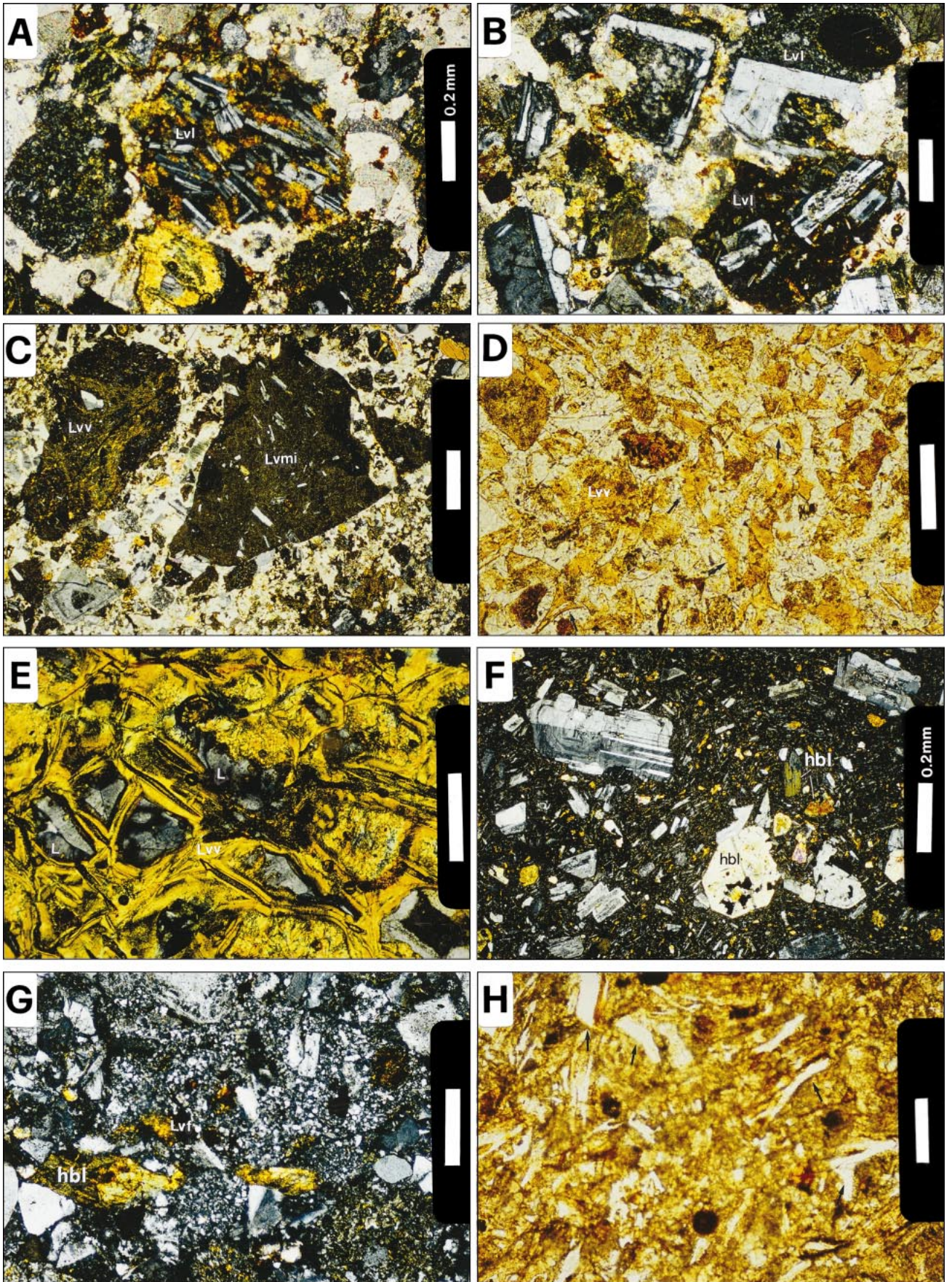
Figure 3. Photomicrographs of grain textures in the tuffaceous sandstone petrofacies of the Gran Cañon Formation. (A–E) Mafic petrofacies. (F–H) Felsic petrofacies. (A and B) Lathwork texture (volcanic lithic grains—Lvl in Fig. 4) of basalt grains with labradorite laths in (A) orange and (B) black vitric groundmass. (C) Microlitic texture (volcanic lithic grains with microlitic texture—Lvmi in Fig. 4) of basalt and basaltic andesite grains, with plagioclase microlites and brown groundmass. (D and E) Vitric volcanic lithic grains (volcanic lithic grains with vitric texture—Lvv in Fig. 4) occur as (C) brown and (D, E) orange glass. (D) Mafic vitric tuff (Lvv; arrows indicate examples of shards). (E) Detail of a basaltic vitric grain (Lvv) with light brown sideromelane largely replaced by orange palagonite and laumontite (L) vesicle filling. (F) Crystal-lithic felsic tuff, with abundant plagioclase and hornblende (hbl). (G) Felsitic granular texture (volcanic lithic grains with felsitic granular and seriate textures—Lvf in Fig. 4) with plagioclase and partially corroded hornblende phenocrysts in a silicic granular groundmass. (H) Felsic vitric tuff with bubble-wall shards (arrows indicate examples of shards). A, B, C, E, F, and G are in cross-polarized light; D and H are in plane-polarized light. White bar length represents 0.2 mm.
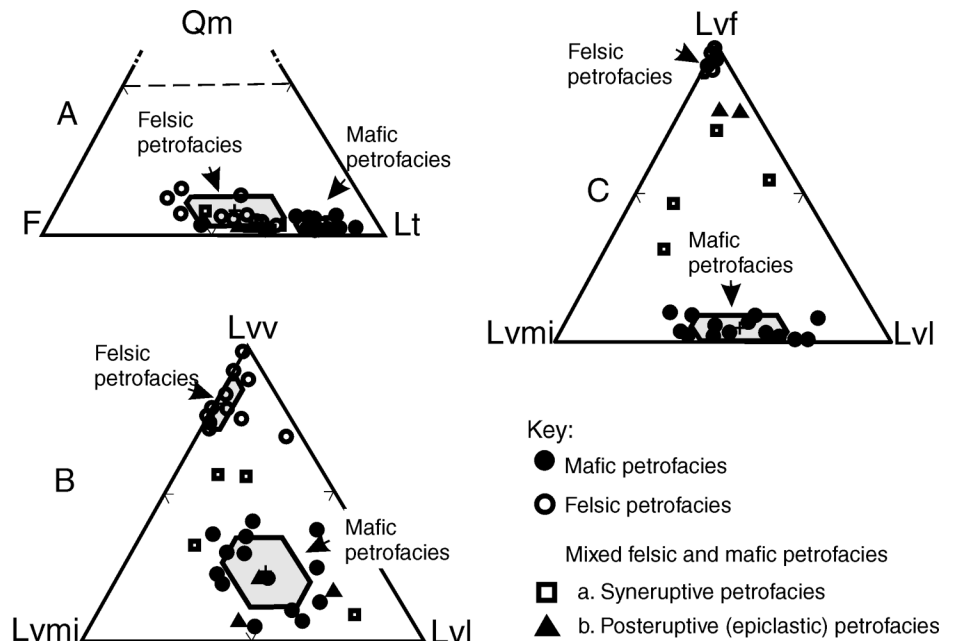

Figure 4. Triangular plots of Gran Cañon Formation tuffaceous sandstone samples: Polygons show mean and standard deviation for felsic and mafic petrofacies. Polygons for the syneruptive mixed petrofacies and the posteruptive mixed petrofacies are not shown because there are so few examples. (A) Qm—monocrystalline quartz, F—feldspars, Lt—fine-grained lithic grains. (B) Lvv—volcanic lithic grains with vitric texture, Lvmi—volcanic lithic grains with microlitic texture, and Lvl—volcanic lithic grains with lathwork texture. (C) Lvf—volcanic lithic grains with felsitic granular and seriate textures, Lvmi—volcanic lithic grains with microlitic texture, and Lvl—volcanic lithic grains with lathwork texture.

sand(stone) suites for which raw data were published or could be obtained from the authors responsible (including our own unpublished raw data). Comparison of the sandstones' compositional modes—including textural proportions—to volcaniclastic sediments of known mafic, intermediate-composition, and felsic provenance (Table DR4; Fig. 5)—suggests that there are two distinct clusters, one more mafic and the other more felsic. The seven samples that plot between the distinct mafic and felsic fields are referred to as mixed felsic + mafic. These compositional groups roughly correlate with Gran Cañon lithofacies; for example, the mafic group is mainly composed of samples from the tuff lithofacies and lapilli-tuff lithofacies, whereas the felsic group correlates with the primary volcanic lithofacies. Because of this stratigraphic connection, we refer to these groups as petrofacies.

Mafic Tuffaceous Sandstone Petrofacies

The mafic tuffaceous sandstone samples consist dominantly of volcanic lithic frag-

ments, largely exhibiting lathwork and microlitic textures and subordinate vitric lithic fragments (Fig. 4, B and C). Single crystals of plagioclase (4.6%–31%) and of clinopyroxene (1%–7%) are less abundant in the mafic samples than they are in the felsic samples (Table DR2—see footnote 1). Basalt clasts range from dense nonvesicular types to highly vesicular scoria fragments and are generally angular to subangular. Every mafic sample has either blocky shards (0.8%–20.8%) or fragments of scoria (0–11.2%) (Table DR2), some of which are blocky. The former are generally considered to be the result of nonexplosive to mildly explosive thermal contraction and shattering of glass in hydrovolcanic to phreatomagmatic eruptions, typical of deep-water volcanism (see references in Heiken and Wohletz, 1985, p. 13). The latter are attributed to magmatic vesiculation during explosive magmatic or phreatomagmatic eruptions (Heiken and Wohletz, 1985).

Felsic Tuffaceous Sandstone Petrofacies

The felsic tuffaceous sandstone samples consist dominantly of felsitic granular lithic

fragments, with lesser vitric lithic fragments (Fig. 4, B and C). On both Figure 4B and Figure 4C, the felsic samples lie in fields entirely separate from the *mafic petrofacies.* Single crystals are more abundant in the felsic samples than in the mafic samples (Fig. 4A) and consist of plagioclase (12.2%–40%), quartz (2.6%–13%), hornblende (0.8–7.2%), and K-feldspar (0%–4%) (Table DR2—see footnote 1). The ratio of unaltered green hornblende to total hornblende is high (0.9–1.0), putting Gran Cañon samples in the range of syneruptive facies as defined by Erskine and Smith (1993) and Smith and Lotosky (1995). Furthermore, a pyroclastic source is indicated by this ratio because unaltered green hornblende is not found in lava flows (Smith and Lotosky, 1995). Like the mafic samples, grains in the felsic samples show little to no evidence of textural modification. Some samples are composed largely of glass.

Every felsic sample has bubble-wall shards or pumice, except for samples we did not point-count from the two fine-grained felsic marker horizons (T1 and T2) near the base of the section, which have dominantly platy shards and bubble-wall shards. The platy
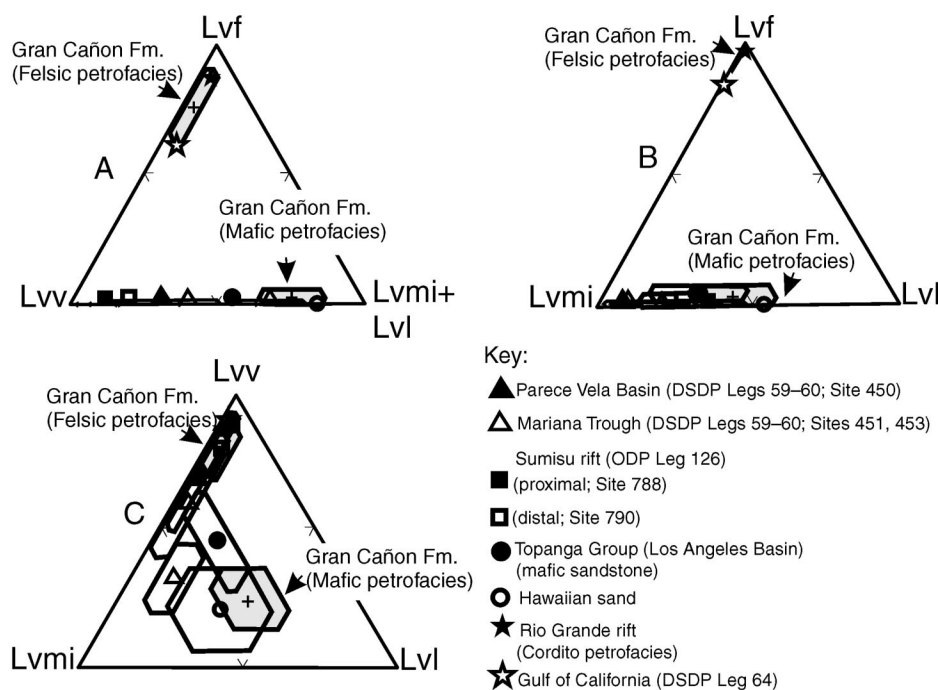
Figure 5. Triangular plot of aphanitic volcanic lithic grains in Gran Cañon Formation tuffaceous sandstone samples, compared with detrital (compositional) modes of mafic, felsic, and mixed felsic + mafic and/or intermediate-composition volcanic provinces from various published sources (Table DR4; see footnote 1). Key shows symbols for mean values. In order to simplify the diagram, only selected fields of variation (polygons defined by one standard deviation on either side of mean) are shown. (A) Lvf–Lvv–(Lvmi + Lvl)—felsitic–vitric–(microlitic + lathwork). (B) Lvf–Lvmi–Lvl—felsitic–microlitic–lathwork. (C) Lvv–Lvmi–Lvl—vitric–microlitic–lathwork. Mafic examples are (1) eruption-fed, hydrovolcanic (blocky nonscoriaceous shards) in the Topanga Group (Critelli and Ingersoll, 1995) and (2) modern beach sands from the island of Hawaii (Marsaglia, 1993). Felsic examples are (1) fluvial volcaniclastic sandstones (Cordito petrofacies) from the Rio Grande rift (Ingersoll, 1984; Ingersoll and Cavazza, 1991) and (2) marine volcaniclastic sands deposited within the Gulf of California (Marsaglia, 1991). Mixed (felsic + mafic) and/or intermediate-composition examples are from DSDP and ODP sites located in the Parece Vela Basin and Mariana Trough (Packer and Ingersoll, 1986; Marsaglia and Devaney, 1995) and an incipient backarc basin (Sumisu rift) in the Izu-Bonin arc (ODP Leg 126 Shipboard Scientific Party, 1989; Nishimura et al., 1992). The synrift sequences drilled in the Sumisu rift are compositionally bimodal (Marsaglia, 1992). Similar compositions characterize synrift sequences in the Mariana backarc basin (Marsaglia and Devaney, 1995).

shards near the base of the section indicate granulation by contact of magma with water (Heiken and Wohletz, 1985). The abundance of pumice and bubble-wall shards in the upper part of the Gran Cañon Formation and the absence of platy or blocky shards indicate explosive magmatic eruptions in the absence of external water.

Mixed Felsic + Mafic Tuffaceous Sandstone Petrofacies: Syneruptive and Posteruptive

The *mixed felsic + mafic petrofacies* can be subdivided into two types, *syneruptive* and

posteruptive, on the basis of the presence or absence of glass (shards, pumice, or scoria), respectively. These syneruptive and posteruptive mixed petrofacies are distinguished best on ternary plots emphasizing volcanic lithic textures (Fig. 4), where it is apparent that the syneruptive samples, generally, contain more vitric lithic grains. The syneruptive mixed petrofacies occurs within the upper third of the pyroclastic apron sequence (in the tuff and lapilli-tuff lithofacies) and contains shards, scoria and pumice shreds (Table DR2—see footnote 1), whereas samples included in the posteruptive mixed petrofacies

are from the epiclastic lithofacies at the top of the Gran Cañon Formation and are typified by mixed compositions as well as a notable lack of shards, pumice, or scoria (Busby-Spera, 1988).

DISCUSSION

Tuff Lithofacies and Lapilli-Tuff Lithofacies

Busby-Spera (1988) interpreted the lapilli-tuff lithofacies to be a more proximal equivalent of the tuff lithofacies of the Arroyo Choyal area and Arroyo Gran Cañon sections, and this understanding is supported by the compositional similarities of these subunits (Figs. 6 and 7). The compositional modes for the Gran Cañon tuff lithofacies and lapilli-tuff lithofacies plot in the undissected-arc field of Dickinson et al. (1983) and the intraoceanic-arc to continental-arc subfields of Marsaglia and Ingersoll (1992) on Qm-F-Lt and Qm-K-P plots (Fig. 6). As shown in Figure 5, the mean volcanic-lithic textural proportions of the lithofacies are most similar to (1) upper Miocene sand from DSDP Site 451 on the remnant arc flank of the active Mariana Basin, (2) Pleistocene(?) sand at ODP Site 787 located in the Izu-Bonin forearc region, and (3) the mafic examples, particularly Hawaiian sand. All three of these sand groups were likely derived from emergent volcanic islands: The Hawaiian samples are modern beach sands; the Site 451 samples are from volcanic-apron facies associated with an at least partly emergent volcanic arc (Klein, 1985; Kroenke et al., 1980); and sand at Site 787 was likely derived via submarine canyon from subaerial mafic to intermediate-composition volcanic flows exposed on the island of Hachijo in the Izu-Bonin arc (Marsaglia, 1992). Thus, the high proportion of microlitic and lathwork volcanic lithic fragments that characterize these lithofacies may be due to some combination of their composition, basalt to basaltic andesite, and proximity to and/or derivation from an emergent eruption center.

Despite the fact that their textural attributes are most similar to sand with mafic and/or intermediate-composition provenance, the presence of quartz and felsitic volcanic lithic fragments in many of those samples precludes a purely mafic source for either the tuff lithofacies or the lapilli-tuff lithofacies. This felsic contribution may have been admixed during eruption or transport, given the presence of discrete interbeds of felsic tuff in this interval (un-point-counted intervals as well as samples GC219 and GC17).
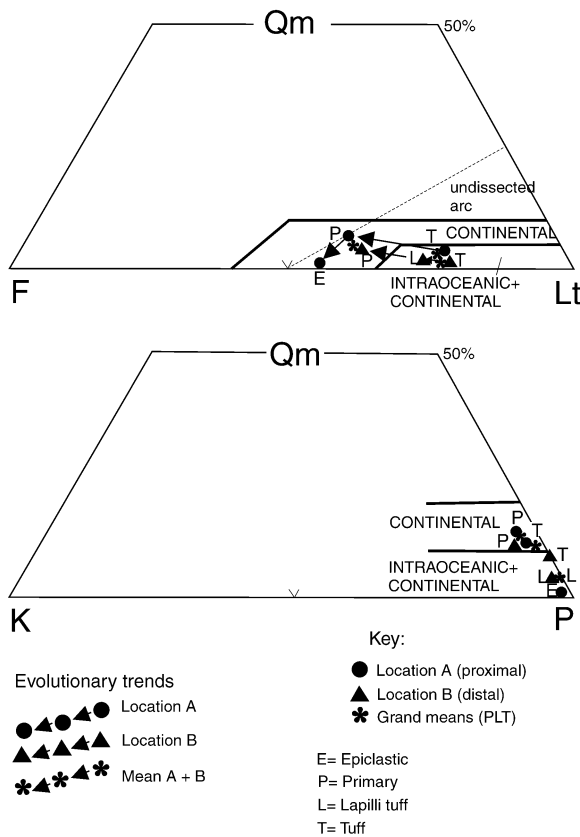
Figure 6. Evolutionary trends from the base to the top of the Gran Cañon Formation: Qm-F-Lt and Qm-K-P diagrams (with superposed provenance field of Dickinson, 1985, and Marsaglia and Ingersoll, 1992).
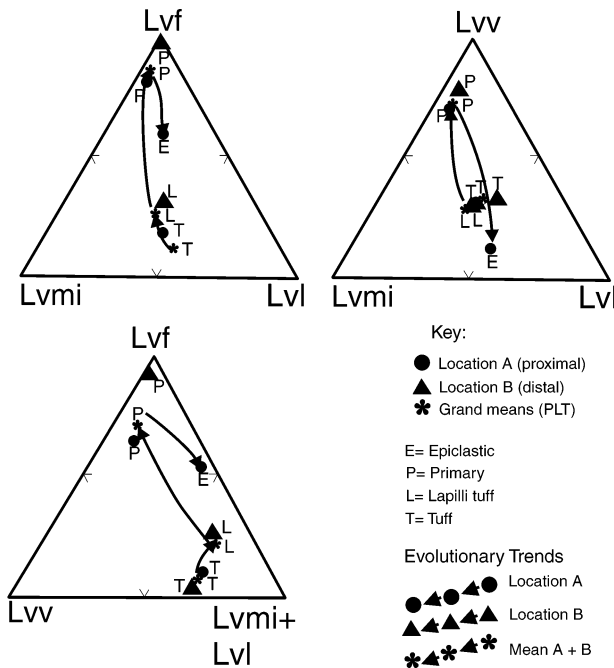

Figure 7. Evolutionary trends from the base to the top of the Gran Cañon Formation: (A) Lvf–Lvmi–Lvl diagram. (B) Lvf–Lvv–(Lvmi + Lvl) diagram. (C) Lvv–Lvmi–Lvl diagram. For explanation of abbreviations, see Figure 5 caption and the text.

Busby-Spera (1988) qualitatively noted an up-section decrease in blocky shards and an up-section increase in scoria fragments in the Gran Cañon Formation, which we can now quantitatively demonstrate in the tuff lithofacies and lapilli-tuff lithofacies (mafic petrofacies) by using modal analysis. To illustrate this trend, we use a discrimination plot proposed by De Rosa (1999) where the axes are JVI (100 × the ratio of juvenile vesiculated glass to total juvenile glass fraction) versus FCrl (100 × the ratio of single [free] juvenile crystals to total juvenile crystals). The Gran Cañon data plot in two distinct groups at extreme values of JVI (high and low) and a range of FCrl values (Fig. 8).

There are several possible causes for the range of FCrl values. De Rosa (1999) related the FCrl to the variability of the initial crystal-size distribution of the fragmenting magma, to the mechanical energy of the eruption, and to transport and depositional effects. De Rosa (1999) argued that the effect of the initial crystal-size distribution is negligible when dealing with sand (2.0–0.0625 mm). The Gran Cañon samples are products of submarine eruptions that were subsequently transported and redeposited into deeper water by turbidity currents. Thus, the variation in their FCrl values is probably a product of sorting and/or mixing during transport.

With respect to JVI values, the Gran Cañon samples exhibit very high and very low vesicularities (Fig. 8). The three highly vesiculated samples were collected in the upper part of the lapilli tuff–tuff breccia lithofacies, in some cases, just below the pillow lavas and breccias of the primary volcanic lithofacies (Fig. 2). Busby-Spera (1988) interpreted this trend as recording a decrease in hydrostatic pressure as the summit of the volcanic source grew nearer to sea level. Those samples with low vesicularity (low JVI) are equivocal in terms of the depth of water in which they formed. Vesiculated glass is commonly produced by CO_2 outgassing of basaltic magma during subaerial eruptions or in water depths of <800 m (Moore and Schilling, 1973; Moore, 1979). Highly vesiculated basaltic breccia has been recovered in the basement rocks of the Sumisu rift (Taylor et al., 1990), which Gill et al. (1990) interpreted as the products of the explosive eruption of H_2O-rich magma in a relatively deep-water (2000 m depth; as suggested by paleontological data) basin formed by arc extension and nascent rifting. As no scoriaceous breccias were noted in the Gran Cañon section, it is more likely that the vesiculated basaltic tuffs in the Gran Cañon accumulated adjacent to a shallowly
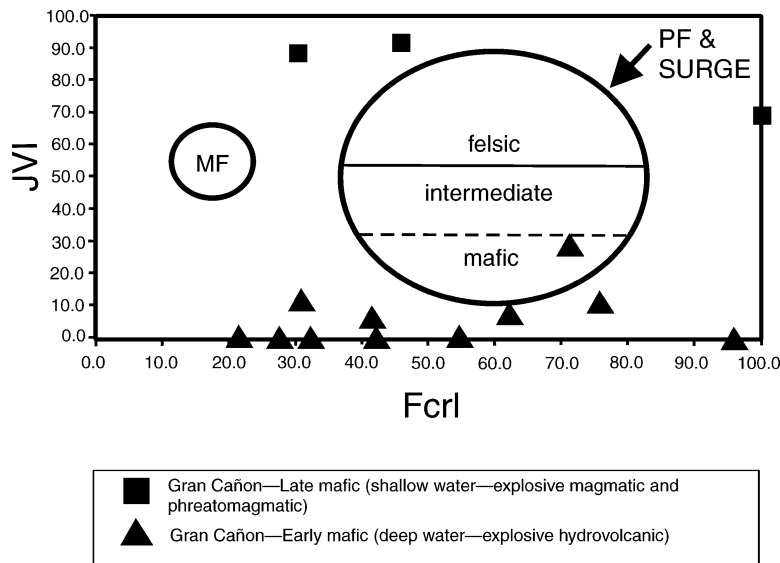
Figure 8. Discrimination plot (proposed by De Rosa, 1999) where the axes are JVI (100 × the ratio of juvenile vesiculated glass to total juvenile glass fraction) vs. FCrl (100 × the ratio of single [free] juvenile crystals to total juvenile crystals). The Gran Cañon data for the mafic petrofacies plot in two distinct groups at extreme values of JVI (high and low) and a range of FCrl values. Our subdivision of the surge deposits into mafic, intermediate-composition, and felsic members is a function of the relative proportion of glass types in each: Mafic (dominantly composed of brown and black glass), intermediate (brown glass dominant, less colorless glass), and felsic (colorless dominant over brown glass). MF represents the explosive magmatic fall field samples, and the PF represents the phreatomagmatic fall field samples.

submerged volcanic center (<800 m depth), as originally interpreted by Busby-Spera (1988). Again, the sedimentary structures in these deposits indicate that the pyroclasts were reworked from where they were produced such that they were transported downslope into deeper water.

Primary Volcanic Lithofacies

Compositional modes for the primary volcanic lithofacies are characterized by (1) higher feldspar (plagioclase and potassium feldspar) and quartz content than the underlying lithofacies (Fig. 6) and (2) volcanic proportions that are dominantly felsitic, with lesser vitric, and microlitic components (Fig. 7). Samples of the primary volcanic lithofacies plot in the undissected-arc field of Dickinson et al. (1983) and the continental-arc subfields of Marsaglia and Ingersoll (1992) on Qm-F-Lt and Qm-K-P plots (Fig. 6); these Gran Cañon samples are unique among deepmarine intraoceanic arc-related sand recovered by DSDP and ODP in their high proportion of felsitic volcanic lithic fragments and quartz. The proportion of felsitic volcanic fragments in the primary volcanic lithofacies is similar to that seen in sand derived from subaerial felsic volcanic provinces (e.g., Rio Grande rift and Sierra Madre Occidental of North America). This result might relate to the more proximal setting interpreted for the primary volcanic lithofacies, as slowly cooling volcanic flows produced more microcrystalline fragments and liberated more quartz phenocrysts.

Higher quartz content in more proximal facies can be seen on the scale of the Gran Cañon outcrop. Compositional modes for tuffaceous sandstone from location A (more proximal facies) are more quartz rich than those of location B (more distal facies) in the Gran Cañon section (Fig. 6), indicating a progressive decrease in quartz away from the source volcanoes (location A to B), a trend that probably continued into more distal basinal settings. Equivalents of these distal facies drilled by DSDP or ODP contain only trace amounts of quartz. Additional support from the rock record includes a study by Gimeno (1994), who reported quartz phenocryst concentrations in proximal epiclastic deposits associated with subaqueous felsic domes. In sum, abundant quartz and felsitic volcanic lithic fragments could be characteristic of proximal felsic volcanic facies not previously

recovered in deep-ocean cores (see discussion in Marsaglia, 1995).

Alternatively, the high quartz content could be attributed to a ''quasi-continental'' more highly evolved magmatic-arc source. Also, given the age of the Gran Cañon Formation and associated degree of burial diagenesis, the felsitic textures could be a product of postburial devitrification or alteration of originally colorless felsic glass, a major component in volcanic sediment produced during arc rifting (Marsaglia, 1992; Marsaglia and Devaney, 1995).

Epiclastic Lithofacies

The compositional modes of sandstone from the epiclastic lithofacies are somewhat unique from underlying units. They plot in the undissected-arc field of Dickinson et al. (1983), and the continental-arc subfields of Marsaglia and Ingersoll (1992) on Qm-F-Lt and Qm-K-P plots (Fig. 6). In addition, they are characterized by relatively high plagioclase (Fig. 6), intermediate felsitic, and low vitric volcanic lithic proportions (Fig. 7) in comparison to other intraoceanic-arc examples. Because of the relatively low quartz content of the epiclastic sandstones, it is unlikely that they were derived from the erosion of underlying more quartzose units.

Summary of Vertical Trends

There are distinct up-section shifts in detrital compositional modes as defined by mean compositions for Gran Cañon lithofacies (Table DR3—see footnote 1). Arrows defining compositional trends are shown in Figures 6 and 7. These trends show that the sand fraction of the Gran Cañon Formation is generally of mafic or intermediate composition in both the tuff lithofacies and lapilli-tuff lithofacies and generally felsic in the primary volcanic lithofacies (Table DR3). The epiclastic lithofacies has a more intermediate composition. This overall compositional trend has important implications for the interpretation of the tectonic evolution of the Gran Cañon arc system, as discussed next.

REFINED TECTONIC MODEL FOR GRAN CAÑON FORMATION

The backarc setting of the Gran Cañon Formation has been inferred, in part, from the petrology and geochemistry of underlying Jurassic basement complexes, particularly the Cedros Island ophiolite. The basement lithology changes northwestward, across the Pinos

syncline (Fig. 1), from the Cedros Island ophiolite to the intraoceanic-arc rocks of the Choyal Formation. Nowhere on Cedros Island is the contact between arc and ophiolite basement exposed, and it probably lies under the Pinos syncline. The compositional similarity of volcaniclastic sequences on the northwestern and southeastern flanks of the Pinos syncline, as determined in this study, suggests that the Gran Cañon Formation is draped across the transition from arc basement to backarc basement, as depicted by Busby-Spera (1988). The fact that the Gran Cañon Formation straddles this crustal boundary helps set limits on the likely depositional setting during the initial stages of sedimentation in the basin, as shown in Figure 9A.

The compositional modes of the tuff lithofacies and lapilli-tuff lithofacies provide insight into the early history of the Gran Cañon magmatic arc (Fig. 9A). The oldest samples examined at location A and location B (Fig. 1) are felsic (GC17) and mafic (GC205a), respectively. We suggest that there was bimodal magmatism during basin inception. Such bimodal magmatism has been documented and suggested for the early-rift and seafloor-spreading phases of modern backarc basins in the western Pacific. For example, Marsaglia and Devaney (1995) found greater quantities of felsic components (colorless glass, quartz, and volcanic lithic fragments with felsitic textures) in synrift sediment in the Mariana region. This pattern has also been observed in the Lau Basin (Clift, 1995; Clift and ODP Leg 135 Scientific Party, 1995) and Sumisu rift (Taylor et al., 1990). The relatively high mean proportion of felsic detritus in the tuff lithofacies and lapilli-tuff lithofacies indicates that the arc volcanoes were somewhat evolved.

The shift from arc basement overlain by proximal facies to backarc ophiolite overlain by more distal facies across the Pinos syncline, as well as the apparent continuous record of volcanism, suggests that rifting occurred behind the arc axis (i.e., backarc rifting). As discussed by Marsaglia and Devaney (1995), forearc rifting results in progressive temporal and spatial shifts in volcanism and associated depocenters in the backarc basin. In contrast, the locus of magmatism is more static in the case of backarc rifting, resulting in the superposition of volcanic centers through time, producing a semicontinuous record on the arc side of the backarc basin (i.e., toward the trench) (Marsaglia and Devaney, 1995). The model depicted in Figure 9 for the Gran Cañon magmatic arc shows initiation of rifting behind the arc axis (backarc). The primary volcanic lithofacies includes basalt flows and coarse felsic tuffs and breccias, indicating more proximal facies of a volcanic center or centers.

In Busby-Spera's (1988) original interpretation of the Gran Cañon Formation, dacite pyroclastic rocks of the primary volcanic lithofacies were inferred to record the eruption of differentiated magmas, which climaxed the growth of the adjacent island arc. Basalt lavas were inferred to have been fed from fissures that extended down the apron within the backarc basin as a form of intraplate volcanism on the "hot," arc side of the basin, unaccompanied by faulting. Drilling in the Izu-Bonin region showed that rifting of the arc and the resultant change in stress regime can be responsible for bimodal volcanism, including the development of silicic calderas (Gill et al., 1992); in the Izu-Bonin case, these calderas provide an abundant supply of dacite pyro-
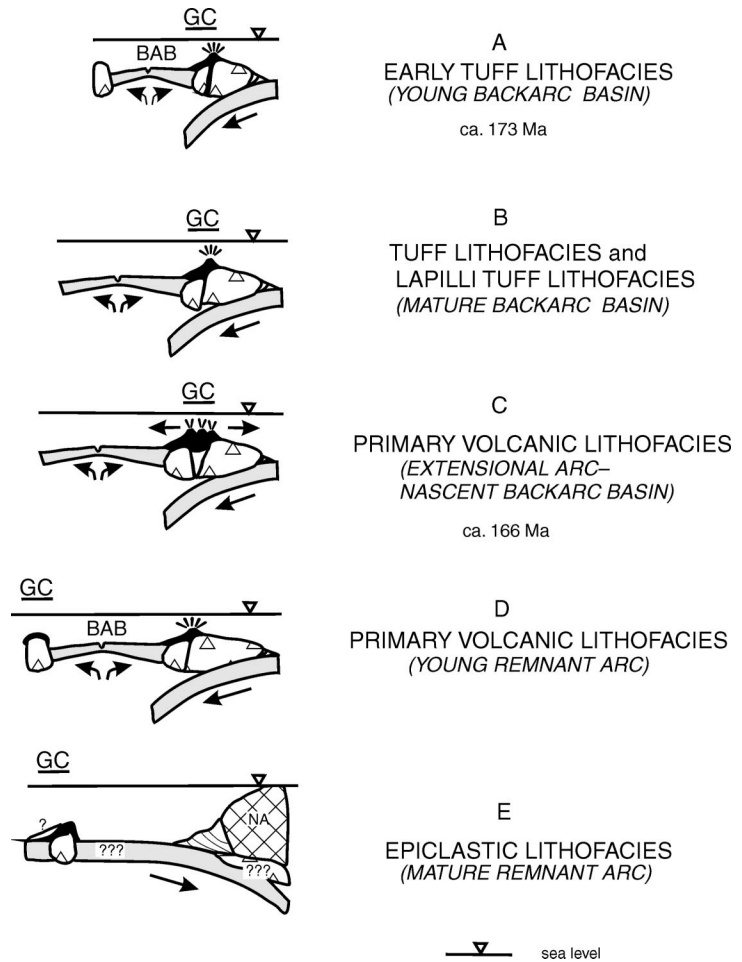

Figure 9. Schematic diagram of the tectonic setting during accumulation of the various lithofacies of the Gran Cañon Formation. Note that volcanoes shown as submerged may have been emergent islands. GC refers to the approximate setting of the Gran Cañon Formation (Cedros Island) in each time frame. Approximate ages for the early tuff and primary volcanic lithofacies are indicated. (A) The oldest samples analyzed above basement are bimodal, suggesting deposition in a nascent backarc (BAB—backarc basin). (B) With continued subduction and seafloor spreading in the backarc basin, the arc matures. (C) Eventually, the arc starts a new extensional phase. The Gran Cañon Formation is rifted away from the frontal arc to form a remnant arc, and magmatism wanes. (D) The extension leads to another phase of backarc-basin formation. (E) Eventually, the remnant arc undergoes thermal subsidence and becomes partly draped by extrabasinal turbidites. Stage E depicts a possible scenario just prior to accretion of the Gran Cañon terrane to the North American continent (NA). The switch in polarity of subduction pictured in D and E requires the frontal arc (shown in A–D) to be removed by either translation or subduction erosion.

clastic debris, which dominates the stratigraphic record of the backarc basin (Nishimura et al., 1991, 1992). Thus, the abundance of dacitic volcanic and pyroclastic debris and the alkalic tholeiitic composition of the basalts in the Gran Cañon Formation are consistent with the interpretation of arc extension.

Based on comparisons with models constructed from DSDP and ODP drilling of Cenozoic examples, we suggest that the up-section shift from tuff of mafic and/or intermediate composition to a bimodal combination of basaltic flows and dacitic pyroclastic rocks indicates that the Gran Cañon arc underwent another rifting episode. Given the constraints of our model for the setting of the lower Gran Cañon Formation (tuff and lapilli tuff) and associated basement rocks, the likely setting during accumulation of the bimodal primary volcanic lithofacies was an arc edifice that was undergoing extension and rifting (Fig. 9C). Evidence of success of this last period of extension, in other words, whether extension progressed to the seafloor-spreading phase (as pictured in Fig. 9D) or ceased, might be found in the overlying sedimentary sequence. Facies recovered across the Mariana Basin (see Marsaglia and Devaney, 1995) show that if extension and rifting progress to seafloor spreading, then the remnant arc becomes isolated from volcaniclastic input, and the cover is largely pelagic. If rifting was not successful, then subduction may have continued, with another phase of magmatic-arc development superimposed on the extended arc.

The composition of sand within the epiclastic lithofacies (high plagioclase content and volcanic fragments exhibiting microlitic and lathwork textures) can be explained in several ways. First, an intermediate-composition source may have been made up of more evolved arc volcanoes; however, the lack of glass-rich pyroclastic-apron facies does not support arc rejuvenation. Likewise, it is unlikely that the epiclastic lithofacies was derived from underlying units or lateral equivalents because it has little compositional affinity with them, particularly with respect to quartz content. If the epiclastic facies was derived from the erosion of underlying units, then one might expect it to be more enriched in quartz than the underlying units as a function of weathering and transport; however, the opposite is true. Last and perhaps most plausible, there is the possibility that these are extrabasinal turbidites later draped onto the subsided remnant arc (Fig. 9E). In Figure 9E, the remnant arc is pictured as an isolated terrane associated with an oceanic plate subducting beneath the North American continent (on the

right). The fate of the frontal-arc part of the Gran Cañon arc system (subducted, translated?) remains equivocal (Fig. 9E).

Faulting obscures the contact of the Gran Cañon with overlying units. We have observed continentally derived coarse-grained detritus in the overlying Upper Jurassic Coloradito and Eugenia Formations, which suggests a much different tectonic setting more proximal to a continental margin (e.g., continental margin to right in Fig. 9D). These formations have been interpreted as recording the docking of the Gran Cañon basement with the North America continent (Boles and Landis, 1984).

SUMMARY AND CONCLUSIONS

Studies of modern backarc basins demonstrate that the history of basin formation and evolution is reflected in the sedimentary fill of the basins, particularly the composition and texture of volcanic and volcaniclastic components. In this study, we show that this history can be deciphered in ancient backarc-basin sequences, even if they are only partly preserved in accreted terranes. Specifically, we refine a tectonic model for the Gran Cañon Formation (Busby-Spera, 1988) by proposing that the primary volcanic lithofacies formed during a second arc rifting event (the first being the creation of the backarc basin). We illustrate this evolution in proximal volcanic facies, thus expanding current models based on distal facies that were more easily cored and recovered during deep-sea drilling.

REFERENCES CITED

Arculus, R.J., Gill, J.B., Cambray, H., Chen, W., and Stern, R.J., 1995, Geochemical evolution of arc systems in the western Pacific: The ash and turbidite record recovered by drilling, *in* Taylor, B., and Natland, J., eds., Active margins and marginal basins of the western Pacific: American Geophysical Union Monograph 88, p. 45–65.

Boles, J.R., and Landis, C.A., 1984, Jurassic sedimentary melange and associate facies Baja California, Mexico: Geological Society of America Bulletin, v. 95, p. 13–21.

Busby-Spera, C.J., 1987, Lithofacies of deep marine basalts emplaced on a Jurassic backarc apron, Baja California (Mexico): Journal of Geology, v. 95, p. 671–686.

Busby-Spera, C.J., 1988, Evolution of a Middle Jurassic back-arc basin, Cedros Island, Baja California: Evidence from a marine volcaniclastic apron: Geological Society of America Bulletin, v. 100, p. 218–233.

Cambray, H., Pubellier, M., Jolivet, L., and Pouclet, A., 1995, Volcanic activity recorded in deep-sea sediments and the geodynamic evolution of western Pacific island arcs, *in* Taylor, B., and Natland, J., eds., Active margins and marginal basins of the western Pacific: American Geophysical Union Monograph 88, p. 97–124.

Clift, P.D., 1995, Volcaniclastic sedimentation and volcanism during the rifting of western Pacific backarc basins, *in* Taylor, B., and Natland, J., eds., Active margins and marginal basins of the western Pacific: American Geophysical Union Monograph 88, p. 67–96.

Clift, P.D., and ODP Leg 135 Scientific Party, 1995, Volcanism and sedimentation in a rifting island-arc terrain: An example from Tonga, southwest Pacific, *in* Smellie, J.L., ed., Volcanism associated with extension at consuming plate margins: Geological Society [London] Special Publication 81, p. 29–51.

Critelli, S., and Ingersoll, R.V., 1995, Interpretation of neovolcanic versus paleovolcanic sand grains: An example from Miocene deep-marine sandstone of the Topanga Group (southern California): Sedimentology, v. 42, p. 783–804.

Critelli, S., and Le Pera, E., 1994, Detrital modes and provenance of Miocene sandstones and modern sands of the southern Apennines thrust-top basins (Italy): Journal of Sedimentary Research, v. 64, p. 824–835.

De Rosa, R., 1999, Compositional modes in the ash fraction of some modern pyroclastic deposits: Their determination and significance: Bulletin of Volcanology, v. 61, p. 162–173.

Dickinson, W.R., 1970, Interpreting detrital modes of graywacke and arkose: Journal of Sedimentary Petrology, v. 40, p. 695–707.

Dickinson, W.R., 1982, Compositions of sandstones in circum-Pacific subduction zones and forearc basins: American Association of Petroleum Geologists Bulletin, v. 63, p. 2–31.

Dickinson, W.R., 1985, Interpreting provenance relations from detrital modes of sandstones, *in* Zuffa, G.G., ed., Provenance of arenites: Dordrecht, Netherlands, D. Reidel, NATO Advanced Study Institute Series 148, p. 333–361.

Dickinson, W.R., 1988, Provenance and sediment dispersal in relation to paleotectonics and paleogeography of sedimentary basins, *in* Kleinspehn, K.L., and Paola, C., eds., New perspectives in basin analysis: New York, Springer-Verlag, p. 3–25.

Dickinson, W.R., and Suczek, C.A., 1979, Plate tectonics and sandstone compositions: American association of Petroleum Geologists Bulletin, v. 63, p. 2164–2182.

Dickinson, W.R., Beard, L.S., Brakenridge, G.R., Erjavec, J.L., Ferguson, R.C., Inman, K.F., Knepp, R.A., Lindberg, F.A., and Ryberg, P.T., 1983, Provenance of North American Phanerozoic sandstones in relation to tectonic setting: Geological Society of America Bulletin, v. 94, p. 222–235.

Erskine, D.W., and Smith, G.A., 1993, Compositional characterization of volcanic products from a primarily sedimentary record: The Oligocene Espinaso Formation, north-central New Mexico: Geological Society of America Bulletin, v. 105, p. 1214–1222.

Fisher, R.V., and Schmincke, H-U., 1984, Pyroclastic rocks: New York, Springer-Verlag, 472 p.

Gill, J.B., Torssander, P., Lapierre, H., Taylor, R., Kaiho, K., Koyama, M., Kusakabe, M., Aitchison, J., Cisowski, S., Dadey, K., Fujioka, K., Klaus, A., Lovell, M., Marsaglia, K., Pezard, P., Taylor, B., and Tazaki, K., 1990, Explosive deep water basalt in the Sumisu backarc rift: Science, v. 248, p. 1214–1217.

Gill, J.B., Seales, C., Thompson, P., Hochstaedter, A.G., and

Dunlap, C., 1992, Petrology and geochemistry of Pliocene–Pleistocene volcanic rocks from the Izu Arc, Leg 126, *in* Taylor, B., Fujioka, K., et al., Proceedings of the Ocean Drilling Program, Scientific results: College Station, Texas, Ocean Drilling Program, v. 126, p. 383–404.

Gimeno, D., 1994, Genesis of crystal-rich epiclastic rocks from subaqueous silicic lava domes: Role of thermal shock on quartz phenocrysts: Sedimentary Geology, v. 90, p. 33–47.

Hawkins, J.W., 1995, Evolution of the Lau Basin—Insights from ODP Leg 135, *in* Taylor, B., and Natland, J., eds., Active margins and marginal basins of the western Pacific: American Geophysical Union Monograph 88, p. 125–173.

Heiken, G., and Wohletz, K., 1985, Volcanic ash: Berkeley, University of California Press, 246 p.

Ingersoll, R.V., 1984, Felsic sand/sandstone within mafic volcanic provinces: Rift sand/sandstone shows no basaltic provenance: Geological Society of America Abstracts with Programs, v. 16, p. 548.

Ingersoll, R.V., and Cavazza, W., 1991, Reconstruction of Oligo–Miocene volcaniclastic dispersal patterns in north-central New Mexico using sandstone petrofacies, *in* Fisher, R.V., and Smith, G.A., eds., Sedimentation in volcanic settings: SEPM (Society for Sedimentary Geology) Special Publication 45, p. 227–236.

Ingersoll, R.V., Bullard, T.F., Ford, R.L., Grimm, J.P., Pickle, J.D., and Sares, S.W., 1984, The effect of grain size on detrital modes: A test of the Gazzi-Dickinson point-counting method: Journal of Sedimentary Petrology, v. 54, p. 103–116.

Karig, D.E., 1983, Temporal relationships between backarc basin formation and arc volcanism with special reference to the Philippine Sea, *in* Hayes, D.E., Tectonic and geologic evolution of southeast Asian seas and islands: American Geophysical Union Monograph 27, p. 318–325.

Kilmer, F.H., 1977, Reconnaissance geology of Cedros Island, Baja California, Mexico: Southern California Academy of Science Bulletin, v. 76, p. 91–98.

Kilmer, F.H., 1984, Geology of Cedros Island, Baja California, Mexico: Arcata, California, Department of Geology, Humboldt State University, 69 p.

Kimbrough, D.L., 1982, Structure, petrology and geochemistry of the Mesozoic paleo-oceanic terranes of Cedros Island and the Vizcaino Peninsula, Baja California Sur, Mexico [Ph.D. thesis]: Santa Barbara, University of California, 395 p.

Kimbrough, D.L., 1984, Paleogeographic significance of the Middle Jurassic Gran Cañon Formation, Cedros Island, Baja California Sur, *in* Frizzell, V.A., Jr., Geology of the California Peninsula: Society of Economic Paleontologists and Mineralogists, Pacific Section, p. 107–118.

Klaus, A., Taylor, B., Moore, G.F., Mackay, M.E., Brown, G.R., Okamura, Y., and Murakami, F., 1992, Structural and stratigraphic evolution of Sumisu Rift, Izu-Bonin arc, *in* Taylor, B., Fujioka, K., et al., Proceeding of the Ocean Drilling Program, Scientific results: College Station, Texas, Ocean Drilling Program, v. 126, p. 555–574.

Klein, G. deV., 1985, The control of depositional depth, tectonic uplift, and volcanism on sedimentation processes in the backarc basins of the western Pacific Ocean: Journal of Geology, v. 93, p. 1–25.

Klein, G. deV., and Lee, Y.I., 1984, A preliminary assessment of geodynamic controls on depositional systems and sandstone diagenesis in back-arc basins, western Pacific Ocean: Tectonophysics, v. 102, p. 119–152.

Kroenke, L., Scott, R., et al., 1980, Initial reports Deep Sea Drilling Project, Leg 59: College Station, Texas, Ocean Drilling Program, 820 p.

Marsaglia, K.M., 1991, Provenance of sands and sandstones from the Gulf of California, a rifted continental arc, *in* Fisher, R.V., and Smith, G.A., eds., Sedimentation in volcanic settings: SEPM (Society for Sedimentary Geology) Special Publication 45, p. 237–248.

Marsaglia, K.M., 1992, Petrography and provenance of volcaniclastic sands recovered from the Izu-Bonin Arc, Leg 126, *in* Taylor, B., Fujioka, K., et al., Proceedings of the Ocean Drilling Program, Scientific results: College Station, Texas, Ocean Drilling Program, v. 126, p. 139–154.

Marsaglia, K.M., 1993, Basaltic island sand provenance, *in* Johnsson, M.J., and Basu, A., eds., Processes controlling the composition of clastic sediments: Geological Society of America Special Paper 284, p. 41–65.

Marsaglia, K.M., 1995, Interarc and backarc basins, *in* Busby, C., and Ingersoll, R.V., eds., Tectonics of sedimentary basins: Oxford, UK, Blackwell Science, p. 299–329.

Marsaglia, K.M., and Devaney, K.A., 1995, Tectonic and magmatic controls on backarc basin sedimentation: The Mariana region reexamined, *in* Taylor, B., ed., Back-arc basins: Tectonics and magmatism: New York, Plenum Press, p. 497–520.

Marsaglia, K.M., and Ingersoll, R.V., 1992, Compositional trends in arc-related, deep-marine sand and sandstone: A reassessment of magmatic-arc provenance: Geological Society of America Bulletin, v. 104, p. 1637–1649.

Marsaglia, K.M., Boggs, S., Jr., Clift, P., Seyedolali, A., and Smith, R., 1995, Sedimentation in western Pacific backarc basins: New insights from recent ODP drilling, *in* Taylor, B, and Natland, J., eds., Active margins and marginal basins of the western Pacific: American Geophysical Union Monograph 88, p. 291–314.

McPhie, J., Doyle, M., and Allen, R., 1993, Volcanic textures. A guide to the interpretation of textures in volcanic rocks: Hobart, Centre for Ore Deposits and Exploration Studies, University of Tasmania, 198 p.

Moore, J.G., 1979, Vesicularity and CO_2 in mid-ocean ridge basalt: Nature, v. 282, p. 250–253.

Moore, J.G., and Schilling, J.-G., 1973, Vesicles, water, and sulfur in Reykjanes Ridge basalts: Contributions to Mineralogy and Petrology, v. 41, p. 105–118.

Nishimura, A., Marsaglia, K.M., Rodolfo, K.S., Colella, A., Hiscott, R.N., Tazaki, K., Janecek, T., Firth, J., Isiminger-Kelso, M., Herman, Y., Gill, J.B., Taylor, R.N., Taylor, B., Fujioka, K., and LEG 126 Shipboard Scientific Party, 1991, Pliocene–Quaternary submarine pumice deposits in the Sumisu Rift, Izu-Bonin Arc, *in* Fisher, R.V., and Smith, G.A., Sedimentation in volcanic settings: SEPM (Society for Sedimentary Geology) Special Publication 45, p. 201–208.

Nishimura, A., Rodolfo, K., Koizumi, A., Gill, J., and Fujioka, K., 1992, Episodic deposition of Pliocene–Pleistocene pumice deposits of Izu-Bonin Arc, Leg 126, *in* Taylor, B., Fujioka, K., et al., Proceedings of the Ocean Drilling Program, Scientific results: College Station, Texas, Ocean Drilling Program, v. 126, p. 3–21.

ODP Leg 126 Shipboard Scientific Party, 1989, Arc volcanism and rifting: Nature, v. 342, p. 18–20.

Packer, B.M., and Ingersoll, R.V., 1986, Provenance and petrology of Deep Sea Drilling Project sands and sandstones from Japan and Mariana forearc and backarc regions: Sedimentary Geology, v. 51, p. 5–28.

Smith, G.A., and Lotosky, J.E., 1995, What factors control the composition of andesitic sand?: Journal of Sedimentary Research, v. 65, p. 91–98.

Tappin, D.R., Bruns, T., and Geist, E.L., 1994, Rifting of the Tonga/Lau Ridge and formation of the Lau backarc basin: Evidence from Site 840 on the Tonga Ridge, *in* Hawkins, J.W., Parson, L.M., Allan, J.F., et al., Proceedings of the Ocean Drilling Program, Scientific results, Leg 135: College Station, Texas, Ocean Drilling Program, v. 135, p. 367–371.

Taylor, B., and Karner, G.D., 1983, On the evolution of marginal basins: Reviews of Geophysics and Space Physics, v. 21, p. 1727–1741.

Taylor, B., and 24 others, 1990, Proceedings of the Ocean Drilling Program, Initial reports, Leg 126, Sites 787–793, Bonin arc-trench system: College Station, Texas, Ocean Drilling Program, v. 126, 1002 p.

Williams, H., Turner, F.J., and Gilbert, C.M., 1954, Petrography. An introduction to the study of rocks in thin sections: San Francisco, W.H. Freeman and Company, 406 p.

Zuffa, G.G., 1985, Optical analyses of arenites: Influence of methodology on compositional results, *in* Zuffa, G.G., ed., Provenance of arenites: Dordrecht, Netherlands, D. Reidel, NATO Advanced Study Institute Series, v. 148, p. 165–189.

Zuffa, G.G., 1987, Unravelling hinterland and offshore paleogeography from deep-water arenites, *in* Leggett, J.K., and Zuffa, G.G., eds., Deep-marine clastic sedimentology: Concepts and case studies: London, Graham and Trotman, p. 39–61.